



**An organic transistor for detecting the oxidation of an
organic sulfur compound at a solid-liquid interface and its
chemical sensing applications**

Journal:	<i>Faraday Discussions</i>
Manuscript ID	FD-ART-08-2023-000149.R1
Article Type:	Paper
Date Submitted by the Author:	01-Oct-2023
Complete List of Authors:	Sasaki, Yui; The University of Tokyo Institute of Industrial Science; JST, PRESTO Zhang, Yijing; The University of Tokyo Institute of Industrial Science Ohshiro, Kohei; The University of Tokyo Institute of Industrial Science Tsuchiya, Kazuhiko; The University of Tokyo Institute of Industrial Science Lyu, Xiaojun; The University of Tokyo Institute of Industrial Science Kamiko, Masao; The University of Tokyo Institute of Industrial Science Ueno, Yoshinori; Toyobo Co.,Ltd., Corporate Research Center Tanaka, Hikaru; Toyobo Co.,Ltd., Corporate Research Center Minami, Tsuyoshi; The University of Tokyo Institute of Industrial Science

ARTICLE

An organic transistor for detecting the oxidation of an organic sulfur compound at a solid-liquid interface and its chemical sensing applications

Received 00th January 20xx,
Accepted 00th January 20xx

DOI: 10.1039/x0xx00000x

Yui Sasaki,^{a,b} Yijing Zhang,^a Kohei Ohshiro,^a Kazuhiko Tsuchiya,^a Xiaojun Lyu,^a Masao Kamiko,^a Yoshinori Ueno,^c Hikaru Tanaka,^c Tsuyoshi Minami^{*a}

The development of chemical sensors has been promoted with an increase in demand, whereas the potential of chemical sensors as devices to monitor organic reactions has not been revealed yet. Thus, we aim to propose a chemical sensor platform for facile monitoring of chemical reactions, especially at a solid-liquid interface. In this study, an extended-gate-type organic field-effect transistor (OFET) has been employed as a platform to detect chemical reactions at an interface between the extended-gate electrode and an aqueous solution. The OFET device functionalized with 4,4'-thiobisbenzenthioi has shown time- and concentration-dependent shifts in transistor characteristics upon adding H₂O₂. In a selectivity test using five oxidant agents, the transistor responses depended on the oxidation of the organic sulfur compound (i.e., 4,4'-thiobisbenzenthioi) stemming from the ability of the oxidant agents. Therefore, the observed changes in the transistor characteristics have suggested the generation of sulfur-oxidized products at the interface. In this regard, the observed responses were caused by the disulfide formation accompanied by the changes in charges at neutral pH conditions. Meanwhile, weak transistor responses derived from the generation of oxygen adducts have been also observed, which were caused by the changes in dipole moments. Indeed, the yields of the oxygen adducts have been revealed by X-ray photoelectron spectroscopy. The monitoring of gradual changes originating from the decrease in the disulfide formation and the increase in the oxygen adducts implied a novel aspect of the OFET device as a platform to simultaneously detect reversible and irreversible reactions at interfaces without using large-sized analytical instruments. Sulfur oxidation by H₂O₂ on the OFET device has been further applied to the indirect monitoring of an enzymatic reaction in the solution. The OFET-based chemical sensor has shown continuous changes with an increase in a substance (i.e., lactate) in the presence of an enzyme (i.e., lactate oxidase), which indicates that the OFET response depends on the H₂O₂ generation through the enzymatic reaction in the solution. In this study, we have clarified the versatility of organic devices as platforms to monitor different chemical reactions using a single detection method.

1. Introduction

The establishment of analytical methods such as nuclear magnetic resonance (NMR), mass spectrometry (MS), Fourier transform infrared spectroscopy (FT-IR), etc. for the identification of chemical structures at solution states has vigorously accelerated not only the material developments¹ but also the clarification of mechanisms in biological systems.² In addition, X-ray photoelectron spectroscopy (XPS) and Raman spectroscopy have been applied to the surface analysis.³ The accuracy of such well-established apparatuses is highly reliable. In contrast, those methods are unsuitable for simple and rapid assessments because of the necessity of large instruments and trained personnel, and time-consuming measurements including pre-treatment processes for samples. Meanwhile, sensors consisting of receptors (to detect stimuli) and transducers (to visualize the detection information) are superior to easily obtaining the stimuli information qualitatively and quantitatively than the abovementioned instrumental analysis, owing to the simple detection methods.⁴ Although sensors have been developed with an increase in demand, their applicability for monitoring chemical reactions (e.g., oxidation and reduction) has not been satisfactorily evaluated yet. Thus, this study aims to propose a sensor device for facile monitoring of chemical reactions. To this end, one of the chemical reactions widely used, the

^a Institute of Industrial Science, The University of Tokyo, 4-6-1 Komaba, Meguro-ku, Tokyo, 153-8505, Japan. E-mail: tminami@g.ecc.u-tokyo.ac.jp

^b JST, PRESTO, 4-1-8 Honcho, Kawaguchi, Saitama, 332-0012, Japan.

^c Corporate Research Center, Toyobo Co., Ltd., 2-1-1 Katata, Otsu, Shiga, 520-0292, Japan.

Electronic Supplementary Information (ESI) available: Fabrication and characterization of the OFET device, synthesis and identification of 1,2-bis(4-((4-(methylthio)phenyl)thio)phenyl)disulfane, characterization of the extended-gate electrode, time-dependency test, selectivity test, surface analysis, EI MS analysis, DFT calculations, XPS analysis, and real-time monitoring of transistor responses in the absence of lactate oxidase. See DOI: 10.1039/x0xx00000x

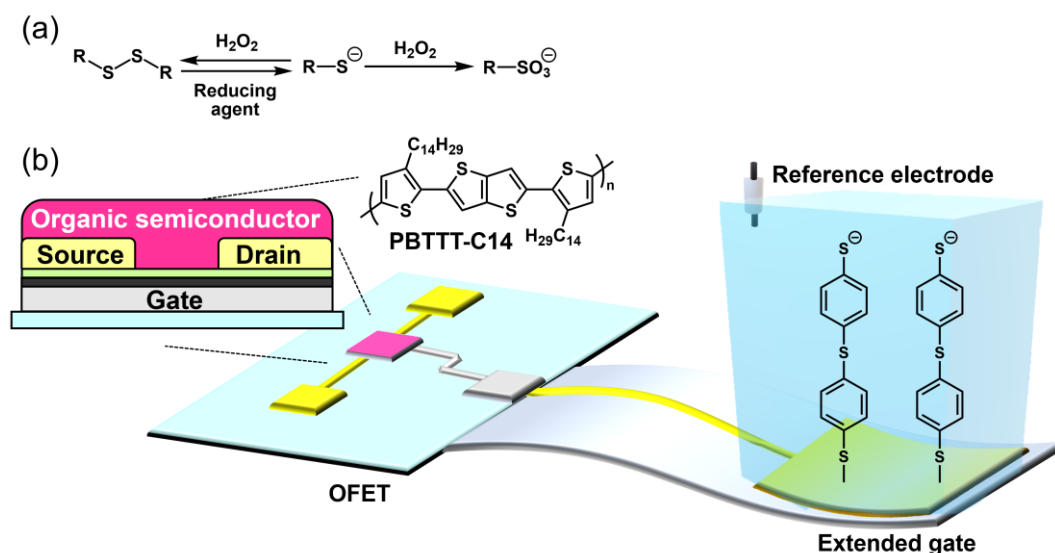


Fig. 1 Scheme of (a) oxidation pathways of an organic sulfur compound with H_2O_2 and (b) the extended-gate-type-OFET device for monitoring the oxidation of an organic sulfur compound (i.e., 4,4'-thiobisbenzenethiol).

oxidation of organic sulfur compounds (i.e., sulfur oxidation) by hydrogen peroxide (H_2O_2)⁵ was selected as the target chemical reaction from the viewpoint of not only high usability in organic synthesis but also significant roles in molecular biology.

In sulfur oxidation by H_2O_2 , the simultaneous formation of disulfide structures and oxygen adducts through different oxidation pathways can be observed (Fig. 1(a)).⁶ In this regard, the difficulty of monitoring sulfur oxidation by H_2O_2 is attributed to simultaneous reversible and irreversible reactions in the oxidation pathways.⁶ In other words, the simultaneous detection of both chemical reactions is required to monitor sulfur oxidation by H_2O_2 . Moreover, the detection of chemical reactions at a solid-liquid interface in situ is challenging in contrast to the analysis of chemical reactions in a solution. Thus, we decided to demonstrate the detection of sulfur oxidation at a solid-liquid interface using an organic field-effect transistor (OFET). OFETs are electronic devices made of solution-processable organic semiconductive materials.⁷⁻¹⁰ The OFETs possessing inherent amplification abilities show switching profiles by applying a gate voltage, and thus the transistor characteristics can be used as sensor signals upon detecting stimuli.^{11, 12} Among device structures, an extended-gate structure that isolates a sensing portion from the operation part (i.e., FET)¹² is appropriate to obtain stable transistor characteristics in stimuli detection at the solid-liquid interface. Since the extended-gate electrode is connected to the gate electrode of the OFET, the changes in surface potentials of the extended-gate electrode affect the conductance of the OFET. As a result, quantitative shifts in transistor characteristics can be observed as changes in conductance corresponding to levels of stimuli (e.g., changes in charges¹³⁻¹⁹ and differences in dipole moments^{20, 21}) on the extended-gate electrode. In this study, 4,4'-thiobisbenzenethiol^{22, 23} was immobilized on an extended-gate gold (Au) electrode as a self-assembled monolayer (SAM) through thiol-gold interactions^{24, 25} (Fig. 1(b)). 4,4'-Thiobisbenzenethiol composed of two phenyl rings can be vertically aligned owing to its rigid skeleton in comparison to alkane dithiols.^{26, 27} On the other hand, a skeleton with shorter molecular length (i.e., 1,4-benzenedithiol) cannot form a SAM vertically aligned because of the adsorption of both terminal thiol groups on the Au surface.^{28, 29} In this oxidation mechanism, we expected that disulfide structures are formed accompanied by the changes in charges upon the addition of H_2O_2 ,^{6, 22} which causes shifts in transistor characteristics. Meanwhile, the generation of oxygen adducts could induce transistor responses derived from the changes in dipole moments on the electrode. Thus, sulfur oxidation manner containing two different oxidation pathways can be detected by a difference in the transistor responses. With sulfur oxidation by H_2O_2 at the interface, the OFET device can be further applied to detect a chemical reaction in the aqueous solution. As sensing applications using sulfur oxidation by H_2O_2 on the extended-gate OFET, we attempted the indirect monitoring of an enzymatic reaction.

2. Experimental

2.1 Materials

All reagents for the fabrication of the extended-gate-type OFET-based device and chemical sensing were used without further purification. Oxidation agents, a dithiol derivative, and a dielectric material purchased from Tokyo Chemical Industry Co., Ltd. were benzoyl peroxide (BPO), 2,3-dichloro-5,6-dicyano-1,4-benzoquinone (DDQ), 1,4-benzenedithiol, tetradecylphosphonic acid (TDPA), and *m*-chloroperoxybenzoic acid (*m*-CPBA). Hydrogen peroxide (H_2O_2), sodium nitrate (NaNO_3), sodium hypochlorite (NaClO), *tert*-butyl hydroperoxide (TBHP), tris(2-carboxyethyl)phosphine hydrochloride (TCEP), Dulbecco's phosphate buffered saline (D-PBS), and dimethyl sulfoxide (super dehydrated) (DMSO) were obtained from FUJIFILM Wako Pure Chemical Industries, Ltd. Methanol

(MeOH), 2-propanol, and sodium chloride (NaCl) obtained from Kanto Chemical Co. Inc. were used for device fabrication and chemical sensing. Poly{2,5-bis(3-tetradecylthiophen-2-yl)thieno[3,2-*b*]thiophene} (PBTTC-14), 1,2-dichlorobenzene, potassium hydroxide (KOH), and lactate oxidase from *Aerococcus viridans* were purchased from Sigma-Aldrich Co. LLC. Reagents for chemical sensing purchased from Alfa Aesar and Dojindo Laboratories Co., Ltd. were sodium lactate and 4-(2-hydroxyethyl)-1-piperazineethanesulfonic acid (HEPES), respectively. Aluminium (Al) wires (1φ) and gold (Au) particles for electrode deposition were obtained from Furuuchi Chemical Co., Ltd., and Tanaka Kikinzoku Kogyo Co., Ltd., respectively. Materials for the OFET fabrication purchased from FUJIKURA KASEI CO., LTD. and Corning, Inc. were silver paste (Dotite, type: D-500) and glass substrates (model Eagle XG, 2 cm×2.5 cm), respectively. An Ag/AgCl reference electrode (model: RE-1B) and a platinum counter electrode were purchased from BAS Inc. Polyethylene naphthalate (PEN) films and 4,4'-thiobisbenzenethiol were supplied from TOYOBO Co., Ltd. A hydrophobic material for the OFET fabrication, CYTOP™ (model CTL-809M) was supplied from AGC Co., Ltd. 1,2-Bis(4-[(4-(methylthio)phenyl)thio]phenyl)disulfane synthesized (See the Electrical Supplementary Information (ESI)).

2.2 Apparatuses

A vacuum thermal deposition apparatus (SVC-700TMSG, Sanyu Electron Co., Ltd.) was performed for the fabrication of metal electrodes. A reactive ion etching (RIE) instrument (SAMCO RIE-10NR) and a UV/O₃ treatment apparatus (ASM401OZ, ASUMI GIKEN Co., Ltd.) were used for surface treatment in device fabrication processes. A spin coating method to form a hydrophobic layer was applied using MIKASA SPINCOATER 1H-D7. All transistor characteristics were assessed by using semiconductor parameter analyzer 4156B, Agilent. For the characterization of the extended-gate electrode, photoelectron yield spectroscopy (PYS) in air (AC-2, Riken Keiki, Co.) was performed to determine the work function of the extended-gate electrode functionalized with 4,4'-thiobisbenzenethiol. Contact angle measurements for the surface wettability test against ultrapure water were performed by using a CA-X contact Angle goniometer (Kyowa interface science Co., Ltd.). The monolayer functionalized on the extended-gate electrode was assigned by Fourier transform infrared spectrophotometry (FT-IR) (a NicoletIS5, Thermo Fisher Scientific Inc.) with a variable angle grazing angle ATR (Harrick Scientific). Elemental analysis was demonstrated by XPS (a PHI Quantera spectrometer, ULVAC-PHI, Inc.). Linear sweep voltammetry (LSV) (an SP-300 potentiostat, Biologic) was applied to estimate molecular densities of SAMs based on Faraday's law, which was operated with five repetitive evaluations from 0 V to -1.5 V at 20 mV/s as the scan rate. The pH conditions of all aqueous solutions were adjusted by using the Seven Excellence pH meter, Mettler-Toledo, Ltd. Electron ionization-mass spectrometry (EI MS) was performed using a JMS-Q1500 from JEOL, and a direct injection probe (DIP). The EI MS was operated by a scan mode with ionization energy at 10 eV, the ionization current at 5 μA, and the ion source temperature at 250 °C. The temperature of the DIP was heated up from 50 to 400 °C during the measurements.

2.3 Fabrication and operation of the OFET device

A gate electrode made of Al (30 nm in thickness) was fabricated on a glass substrate through vacuum thermal evaporation along with a shadow metal mask. The glass substrate for device fabrication was treated with a piranha solution (H₂SO₄:H₂O₂ = 3:1 (v/v)). Subsequently, the surface of the Al gate electrode was activated by a reactive ion etching (RIE) process, followed by the formation of an Al oxide (AlO_x) layer. Afterward, a hydrophobic polymer material (i.e., CYTOP™, CLT-809M in CT-Solv180, ratio 1:1 (v/v)) was entirely covered on the substrate by a spin coating process for fabrication of a bank layer, and the treated substrate was baked at 110 °C for 30 min in an inert gas atmosphere. Next, the RIE process was performed to fabricate a bank layer made of the hydrophobic polymer. After this period, the substrate was immersed in a 2-propanol solution containing TDPA³⁰ (10 mM) for 15 h at room temperature. After washing the substrate with 2-propanol and drying it with the nitrogen (N₂) flow, the substrate was baked at 110 °C for 30 min. In addition, the vacuum thermal evaporation instrument with a shadow metal mask was applied to fabricate source and drain electrodes made of Au (30 nm in thickness). A polymer semiconductive material, PBTTC-14³¹ in 1,2-dichlorobenzene (0.010 wt%) was drop cast on a channel region of the OFET device (width: 50 μm and length: 1000 μm) in an inert gas atmosphere, followed by backing at 160 °C for 10 min. Finally, the surface of the substrate was evenly coated by the CYTOP™ solution, which was baked at 110 °C for 10 min to form a passivation layer for stable device operation under ambient conditions (Fig. S1).

The manufactured OFET was connected to an extended-gate electrode using a conductive cable for chemical sensing, of which gate voltage was applied through the reference Ag/AgCl electrode. The transfer characteristics were obtained by scanning at 0.5 to -3 V as gate voltage (V_{GS}) and -2 V as drain-source voltage (V_{DS}), while the output characteristics were recorded at 0 to -3 V (step: -1 V) as V_{GS} and 0 to -3 V as V_{DS} (Fig. S2).

2.4 Fabrication of the extended-gate electrode

The extended-gate Au electrode (15 mm² of area, 100 nm in thickness) was fabricated on a PEN film by vacuum thermal deposition. The extended-gate electrode was immersed into a DMSO solution containing 4,4'-thiobisbenzenethiol (1 mM) and TCEP (5 mM) for 72 h under ambient conditions, which was washed with MeOH and dried with N₂ gas. In addition, 4-[(4-(methylthio)phenyl)thio]benzenethiol was immobilized by the immersion of the extended-gate electrode into a DMSO solution containing the disulfide material (1 mM) and TCEP (5 mM) for 72 h under ambient conditions, which was washed with MeOH and dried with N₂ gas. Moreover, 1,4-benzendithiol was modified on the extended-gate electrode by immersion into a MeOH solution

containing the dithiol derivative (1 mM) and TCEP (5 mM) for 24 h under ambient conditions, which was washed with MeOH and dried with N₂ gas.

3. Results and Discussion

3.1 Characterization of the extended-gate electrode before and after immobilization of 4,4'-thiobisbenzenethiol

The extended-gate electrode functionalized with 4,4'-thiobisbenzenethiol was qualitatively and quantitatively characterized by using several methods. The molecular density of 4,4'-thiobisbenzenethiol modified on the extended-gate electrode was determined to be $(0.9 \pm 0.2) \times 10^{-9}$ mol/cm² ($n = 3$) by LSV, which indicated that uniform and reproducible functionalization of the SAM was achieved (Fig. 2(a)). In addition, the results of PYS measurements showed the change in the work function of the extended-gate Au electrode before (4.8 eV) and after immobilization of 4,4'-thiobisbenzenethiol (5.0 eV) (Fig. 2(b)). Moreover, an elemental analysis result containing three peaks was observed by XPS measurement, which was derived from three states of sulfur of 4,4'-thiobisbenzenethiol (Fig. 2(c)).²² In a wettability test, water contact angles on the Au electrode showed a change before (59°) and after immobilization of 4,4'-thiobisbenzenethiol (89°), which suggested that a hydrophobic monolayer was functionalized on the surface of the extended-gate Au electrode (Fig. 2(d)). Furthermore, the result of FT-IR(ATR) measurements indicated peaks derived from C-C stretching (1642 cm⁻¹) and C-H bending (876, 1012–1128 cm⁻¹) (Fig. S6). The modification of 4,4'-thiobisbenzenethiol was assessed by the above-mentioned characterization, and thus the detection of the oxidation reaction was subsequently performed in combination with the OFET device.

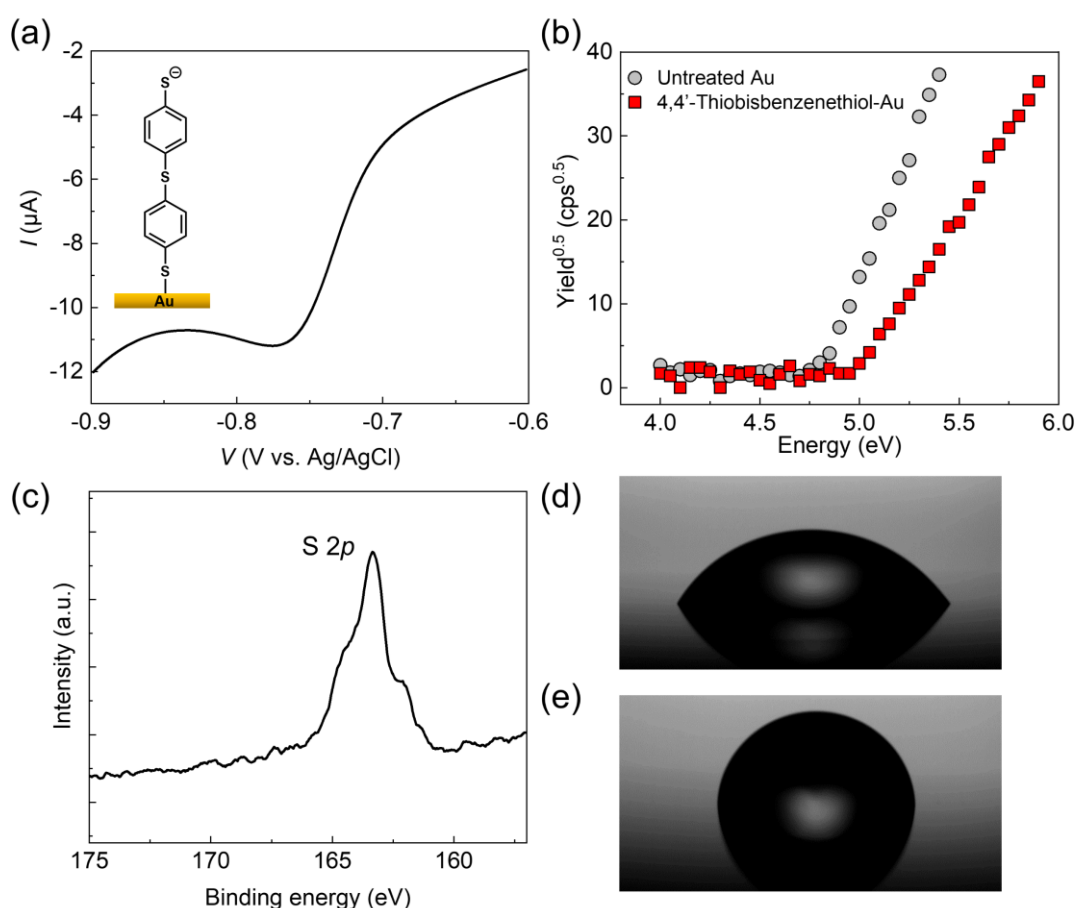


Fig. 2 Characterization results of the extended-gate electrode functionalized with 4,4'-thiobisbenzenethiol. (a) Estimation of the molecular density of 4,4'-thiobisbenzenethiol on the extended-gate Au electrode by LSV in a KOH solution (0.1 M) at 0 V to -1.5 V (scan rate: 20 mV/s). (b) The work function of the untreated Au electrode (gray circle) and the Au electrode functionalized with 4,4'-thiobisbenzenethiol (red square). (c) XPS analysis of the extended-gate Au electrode functionalized with 4,4'-thiobisbenzenethiol. The water contact angle of the extended-gate Au electrode (d) before and (e) after the modification of 4,4'-thiobisbenzenethiol.

3.2 Evaluation of transistor characteristics of the OFET functionalized with 4,4'-thiobisbenzenethiol

The transistor characteristics of the extended-gate-type OFET device functionalized with 4,4'-thiobisbenzenethiol was evaluated in 100 mM HEPES buffer with 100 mM NaCl at pH 7.4. As shown in Fig. S7, the OFET device showed gradual shifts in the transfer curves upon adding H₂O₂ (100 μM). A saturation curve was constructed by a correlation between the transistor response and its response time, which suggested that the OFET device was capable of detecting the time-dependent oxidation reaction (Fig. S7 (b)). Using the time-course change of the threshold voltages (Fig. S7b), the correlation between the reaction time and the concentrations was obtained (Fig. S8) for the estimation of an apparent reaction rate constant. The details are summarized in the ESI. Next, a concentration-dependency of sulfur oxidation was investigated by titration of H₂O₂ using the OFET device functionalized with 4,4'-thiobisbenzenethiol. According to the saturation time in the time-dependency test, the transistor characteristics at each H₂O₂ concentration were recorded at an interval of 10 min. Fig. 3(a) exhibited quantitative changes in the transfer curves corresponding to an increase in H₂O₂ concentration. A non-linear titration isotherm was obtained by collecting threshold voltages (V_{THS}) at different H₂O₂ concentrations (Fig. 3(b)), which suggested that the OFET device enabled the detection of the concentration-dependent oxidation reaction at micromolar levels.

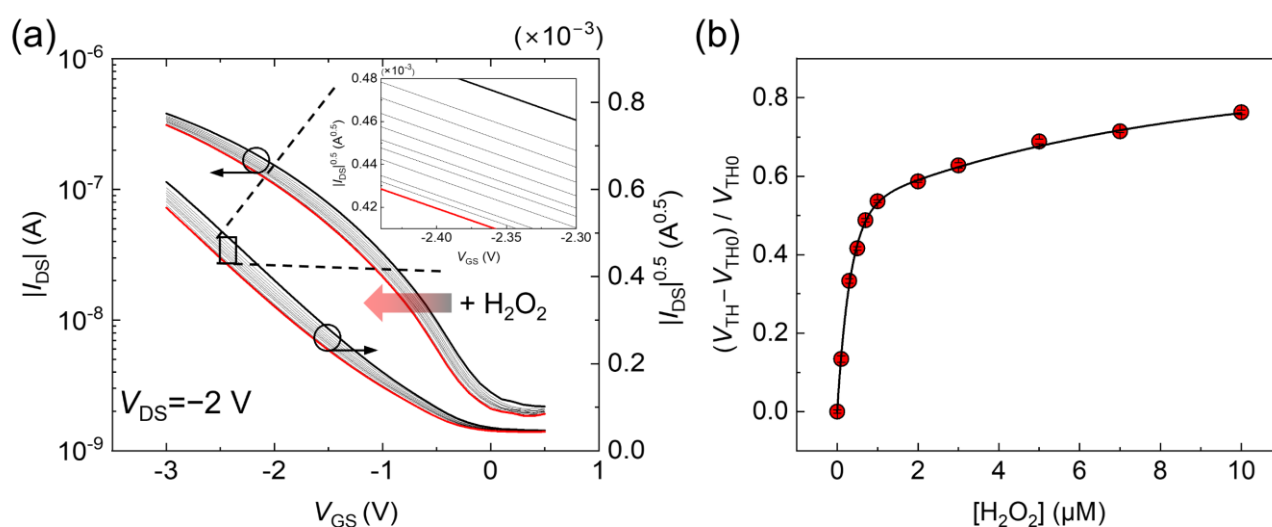


Fig. 3 (a) Transfer characteristics of the OFET device functionalized with 4,4'-thiobisbenzenethiol upon the addition of H₂O₂ in a HEPES (100 mM) buffer solution containing NaCl (100 mM) at pH 7.4. [H₂O₂] = 0–10 μM. (b) The correlation between the V_{TH} changes and H₂O₂ concentrations. The V_{TH0} and V_{TH} mean threshold voltages before and after adding H₂O₂, respectively.

3.3 Selectivity test

The transistor characteristics of the OFET device upon sulfur oxidation by a difference in oxidant agents were evaluated using NaNO₃, NaClO, TBHP, BPO, DDQ, and *m*-CPBA. Fig. 4 shows the highest transistor response to H₂O₂, which depended on the sufficient oxidizing power to 4,4'-thiobisbenzenethiol owing to effective oxygens over other oxidants.⁵ For example, a weaker response to TBHP than H₂O₂ was derived from the inherent moderate oxidizing power for sulfur oxidation. Given sulfur oxidation was not observed in a catalytic oxidation reaction using DDQ in a previous report³², almost no transistor response to DDQ can be concluded to as a reasonable result. Overall, the difference in the transistor responses depended on yields of sulfur oxidation stemmed from the power of the oxidant agents, which suggested the possibility of monitoring a difference in the reactivity of reagents.

3.4 Investigation of the detection mechanism of transistor responses upon sulfur oxidation

According to a previous report, only terminal groups in 4,4'-thiobisbenzenethiol can be oxidized by H₂O₂.⁵ In addition, the oxidation process is accelerated by the anionic form of thiol groups.⁶ Considering the pKa of 4,4'-thiobisbenzenethiol, the terminal thiol groups are deprotonated at pH 7.4.⁶ Thus, we hypothesized that the shifts of transistor characteristics were caused by the conversion of the thiol group into a disulfide structure. Indeed, the results of EI MS analysis supported the conversion of the thiol structure (Fig. S16) into the disulfide structure by adding H₂O₂ (Fig. S17). Moreover, the oxidation mechanism causing the changes in transistor characteristics was investigated by using 1,4-benzenedithiol^{28, 29} and 4-[[4-(methylthio)phenyl]thio]benzenethiol. Because both terminal thiol groups of 1,4-benzenedithiol adsorb on the Au surface,^{28, 29} the extended-gate electrode functionalized with 1,4-benzenedithiol was employed to reveal the effects of transistor responses by the sulfur atoms linked to the Au surface in the oxidation reaction. Fig. 5 showed almost no response of the OFET device to H₂O₂, which implied that the sulfur atoms linked

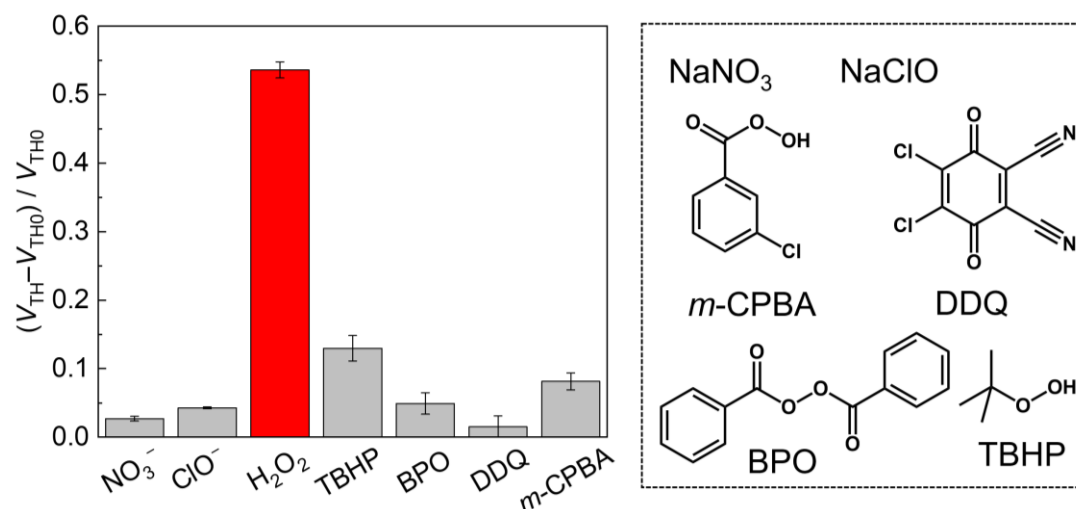


Fig. 4 Selectivity test against seven oxidants in HEPES (100 mM) buffer solution containing NaCl (100 mM) at pH 7.4. [Oxidant agent] = 1 μM .

to the extended-gate Au electrode did not contribute to causing transistor responses in the oxidation reaction. In addition, a very weak response of the OFET device functionalized with 4-[[4-(methylthio)phenyl]thio]benzenethiol was probably due to changes in dipole moments^{20, 33} originating from the partial formation of the sulfoxide structure (Fig. S18).⁵

Next, a cycle test was performed by using the OFET device functionalized with 4,4'-thiobisbenzenethiol to clarify the detection mechanism based on the dynamic sulfur bonds. In this assay, transistor characteristics upon oxidation with H_2O_2 and reduction with TCEP were recorded alternatively (Fig. 6). Each transistor response at the oxidation process was obtained after immersion of the extended-gate electrode functionalized with 4,4'-thiobisbenzenethiol into an aqueous solution containing H_2O_2 (1 μM) for 10 min. Meanwhile, the same electrode was further immersed into an aqueous solution containing TCEP (1 mM) for 30 min to perform the reduction of the disulfide structures. The treated electrode was rinsed with DI water before measurements of the transistor responses. The abovementioned process was alternatively performed using a single extended-gate electrode. As shown in Fig. 6, alternative changes in V_{TH} values were observed in each treatment process, while the V_{TH} changes gradually decreased with the treatment cycles. Notably, the shifts in the V_{TH} values at the H_2O_2 treatment and the reduction process showed linearity with an increase in the cycle numbers, which can be explained by the sulfur oxidation pathways. As shown in Fig. 1(a), the formation of disulfide structures and oxygen adducts simultaneously proceeds by adding H_2O_2 .⁶ The disulfide formation causes negative shifts in transfer curves owing to the changes in the charges. In contrast, the formation of oxygen adducts induces a weak transistor

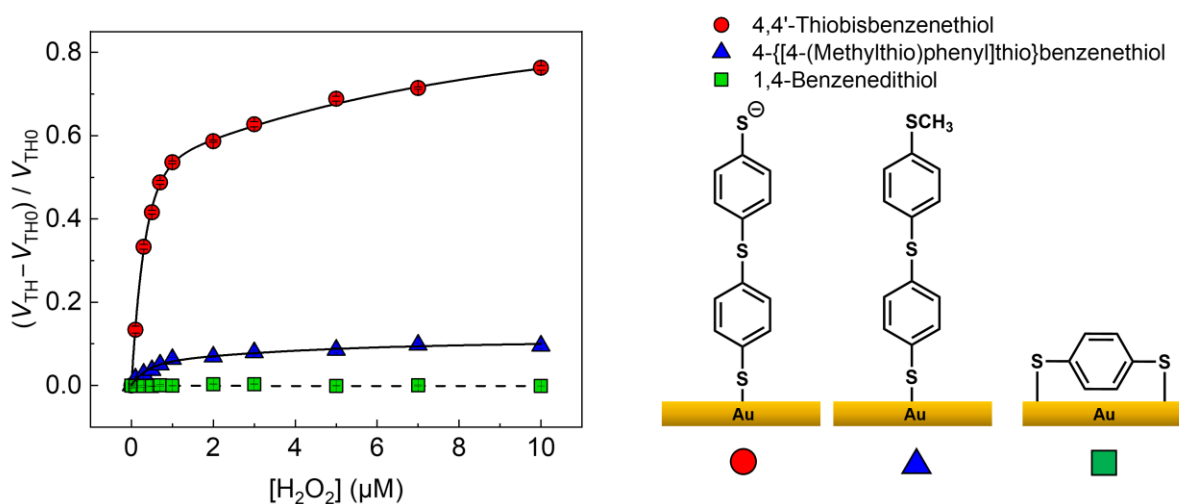


Fig. 5 Each transistor response of the OFET functionalized with 4,4'-thiobisbenzenethiol (red circles), 4-[[4-(methylthio)phenyl]thio]benzenethiol (blue triangles), and 1,4-benzenedithiol (green squares) to H_2O_2 in HEPES (100 mM) solution buffer solution containing NaCl (100 mM) at pH 7.4. [H_2O_2] = 0-10 μM .

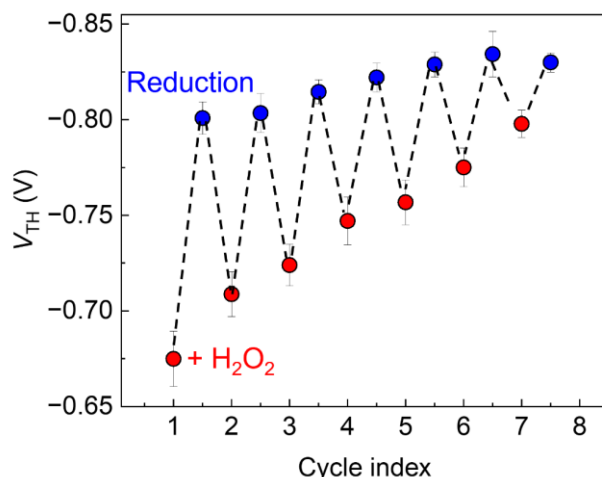


Fig. 6 The cycle test based on dynamic sulfur bonds. Each transistor characteristics upon oxidation with H_2O_2 (1 μM) and reduction with TCEP (1 mM) were recorded alternatively. All experiments were performed in the HEPES buffer (100 mM) containing NaCl (100 mM) at pH 7.4.

response because this oxidation pathway causes a change in the dipole moment. Therefore, the decrease in the changes in V_{TH} with the cycle numbers indicated an increase in oxygen adducts as well as a decrease in disulfide formation. Certainly, the increase in oxygen concentrations of the 4,4'-thiobisbenzenethiol-modified Au electrode by H_2O_2 treatment was revealed by XPS analysis, which supported the formation of oxygen adducts in sulfur oxidation (Fig. S19). This demonstration clarified that the transistor responses depended on the generation of products in each oxidation pathway, which implied the potential of the OFET device allowing the simultaneous detection of reversible and irreversible chemical reactions without using conventional instrumental analysis.

3.5. Evaluation of detectability of H_2O_2 as a chemical sensor

From the viewpoint of chemical sensing of H_2O_2 , H_2O_2 is an essential biomarker to indicate the states of oxidative stress causing Parkinson's disease³⁴, Alzheimer's disease³⁵, cardiac disease³⁶, etc. In the development of chemical sensing for H_2O_2 , the introduction of enzyme-catalyzed reactions into detection portions enables selective and sensitive detection of H_2O_2 ,³⁷ while fluctuation of sensor responses by interference effects of oxygen dissolved in sensing media³⁸ is a bottleneck for quantitative analysis. Given the demand for non-enzymatic H_2O_2 chemical sensors to obtain accurate sensing results, we decided to further evaluate the ability of the manufactured OFET device as a chemical sensor for H_2O_2 . In the H_2O_2 titration (Fig. 3), the limit of

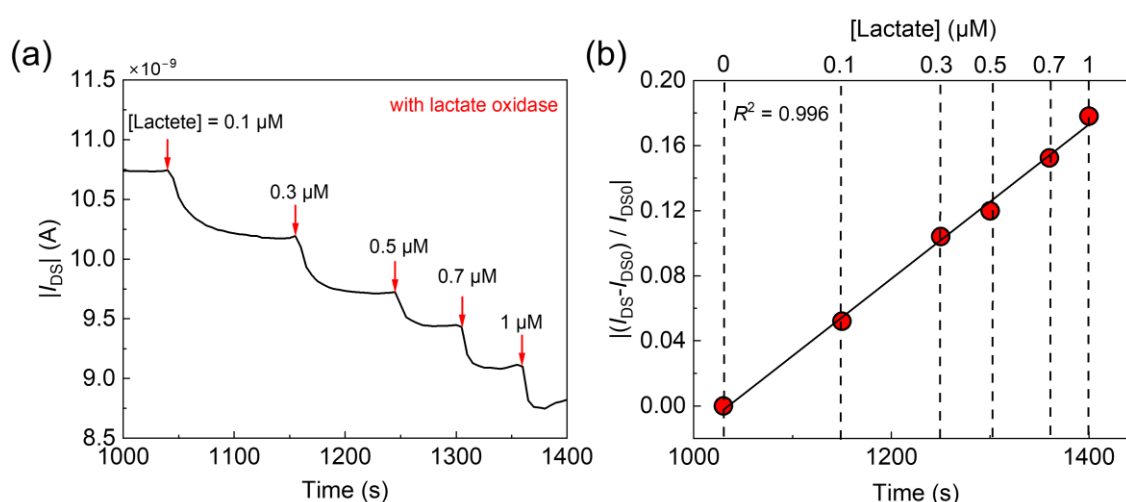


Fig. 7 (a) Real-time monitoring of transistor responses upon adding lactate in the presence of lactate oxidase in a D-PBS solution. [Lactate oxidase] = 0.03 mg/L, [lactate] = 0–1 μM . $V_{\text{GS}} = V_{\text{DS}} = -2$ V. (b) The time- and concentration-dependent V_{TH} changes with an increase in lactate concentration.

detection (LoD) of the OFET device functionalized with 4,4'-thiobisbenzenethiol was estimated to be 50 nM (1.7 ppb) based on the 3σ method³⁹, which indicated higher sensitivity over conventional non-enzymatic chemical sensors based on optical methods⁴⁰⁻⁴² and electrochemical methods.^{38, 43} The obtained favorable sensitivity of the extended-gate-type OFET for H₂O₂ is probably due to the synergy effect of an inherent amplification ability of the OFET and the chemical reaction that occurred at the electrode vicinity.

As a further attempt, we decided to apply the sulfur oxidation system with H₂O₂ incorporated into the extended-gate-type OFET device to indirectly monitor an enzymatic reaction through the change in transistor responses. In the enzymatic reaction using lactate oxidase as an enzyme and lactate as a substance, H₂O₂ is yielded as a product.⁴⁴ In this assay, 4,4'-thiobisbenzenethiol-modified OFET was used as an H₂O₂ sensor to detect the product levels in the enzyme reaction. As shown in Fig. 7(a), the continuous concentration-dependent changes in drain currents were observed with an increase in lactate concentration in the presence of lactate oxidase. Indeed, the transistor response was not obtained in the absence of lactate oxidase, which supported that the observed changes in the transistor characteristics were derived from the yields of H₂O₂ by the enzymatic reaction (Fig. S20). In addition, the transistor responses upon the enzymatic reaction showed a linear-like correlation between the lactate concentrations and the changes in drain currents (Fig. 7(b)), suggesting the potential of the OFET device as the chemical sensor allowing the quantification of H₂O₂ levels in enzymatic reactions at solution states. In fact, the calculated reaction time to accomplish the enzymatic reaction at each lactate concentration based on a previously reported reaction rate of lactate oxidase⁴⁵ was almost matched with the response time of the OFET-based sensor, meaning that produced H₂O₂ was immediately detected by the OFET. Thus, the OFET enables real-time monitoring of H₂O₂ concentrations generated by the enzyme *in situ*. Furthermore, we performed real-time monitoring in the presence of an interferent (i.e., human serum albumin). The protein concentration was decided based on the actual concentration in human saliva. As shown in Figure SX, the continuous changes in the drain current were observed with an increase in lactate concentration, which indicated the monitoring ability of the OFET functionalized with 4,4'-thiobisbenzenethiol even in the presence of excess amount of proteins.

Conclusions

Oxidation of organic sulfur compounds by H₂O₂ is not only widely used in organic synthesis but also plays crucial roles in biological systems. This sulfur oxidation manners contain the simultaneous generation of the disulfide structure and oxygen adducts through different oxidation pathways. Thus, monitoring sulfur oxidation by H₂O₂ is challenging owing to the difficulty of the simultaneous detection of reversible and irreversible reactions. In addition, the establishment of analytical methods for organic reactions at a solid-liquid interface *in situ* is desirable. Herein, we decided to demonstrate the simultaneous detection of reversible and irreversible sulfur oxidation by H₂O₂ using an extended-gate-type OFET device functionalized with 4,4'-thiobisbenzenethiol. The 4,4'-thiobisbenzenethiol-modified OFET showed time- and concentration-dependent transistor responses upon adding H₂O₂, which was derived from the formation of disulfide structures accompanied by the changes in charges. In addition, the selectivity test result against various oxidant agents suggested that the obtained transistor responses upon sulfur oxidation relied on the oxidizing power of oxidant agents. Next, the detection mechanism of the OFET device was investigated by using two derivatives (i.e., 1,4-benzenedithiol and 4-[[4-(methylthio)phenyl]thio]benzenethiol). Almost no response of the OFET functionalized with 1,4-benzenedithiol to H₂O₂ indicated that low contribution of the sulfur atoms linked to the Au surface to inducing transistor responses. Meanwhile, the OFET functionalized with 4-[[4-(methylthio)phenyl]thio]benzenethiol showed a very weak response to H₂O₂, which was presumably due to the change in a dipole moment originating from the formation of oxygen adducts. In a cycle test based on dynamic sulfur bonds, the alternative changes in the V_{TH} values upon oxidation with H₂O₂ and reduction with TCEP supported the formation of disulfide structures, while the decrease in the V_{TH} changes indicated the generation of oxygen adducts as well as the decrease in the disulfide formation. The observed trend of the transistor response originating from the generation of the disulfide structure and oxygen adducts implied the success in the simultaneous detection of both reversible and irreversible sulfur oxidation reactions at the interface. Finally, the ability of the OFET device with 4,4'-thiobisbenzenethiol was extended to chemical sensing for the indirect monitoring of an enzymatic reaction at a solution state. The OFET-based chemical sensor based on sulfur oxidation with H₂O₂ showed the quantitative changes in drain currents upon adding a substance (i.e., lactate) in the presence of an enzyme (i.e., lactate oxidase). The transistor response was derived from the detection of H₂O₂ as a product in the enzymatic reaction, which suggested a concentration-dependent change. Although further investigation and discussion to deeply understand the oxidation reaction at the interface is required, we revealed that the combination of OFETs and appropriate SAM materials will maximize the versatility of organic devices.

Conflicts of interest

There are no conflicts of interest to declare.

Acknowledgements

T. Minami gratefully acknowledges the financial support from the Japan Society for the Promotion of Science (JSPS KAKENHI Grant Nos. JP23H03864 and JP21H01780) and JST CREST (Grant No. JPMJCR2011). Y. Sasaki thanks JSPS KAKENHI (Grant No. JP22K14706). K. Ohshiro and X. Lyu thank the JSPS Research Fellow for Young Scientists (DC1) (Grant Nos. JP23KJ0785 and JP22J23435).

References

- D. A. Skoog, F. J. Holler and S. R. Crouch, *Principles of Instrumental Analysis*, Cengage Learning, 2017.
- T. V. Mishanina, M. Libiad and R. Banerjee, *Nat. Chem. Biol.*, 2015, **11**, 457-464.
- Y. Wang, L. Gan, H. Chen, S. Dong and J. Wang, *J. Phys. Chem. B*, 2006, **110**, 20418-20425.
- A. Hulanicki, S. Glab and F. Ingman, *Pure Appl. Chem.*, 1991, **63**, 1247-1250.
- K. Sato, M. Hyodo, M. Aoki, X.-Q. Zheng and R. Noyori, *Tetrahedron*, 2001, **57**, 2469-2476.
- L. A. H. van Bergen, G. Roos and F. De Proft, *J. Phys. Chem. A*, 2014, **118**, 6078-6084.
- H. Li, W. Shi, J. Song, H.-J. Jang, J. Dailey, J. Yu and H. E. Katz, *Chem. Rev.*, 2019, **119**, 3-35.
- H. Klauk, *Chem. Soc. Rev.*, 2010, **39**, 2643-2666.
- H. Sirringhaus, *Adv. Mater.*, 2005, **17**, 2411-2425.
- F. Wudl, *Faraday Discuss.*, 2014, **174**, 9-20.
- M. L. Hammock, A. Chortos, B. C.-K. Tee, J. B.-H. Tok and Z. Bao, *Adv. Mater.*, 2013, **25**, 5997-6038.
- R. Kubota, Y. Sasaki, T. Minamiki and T. Minami, *ACS Sens.*, 2019, **4**, 2571-2587.
- T. Minami, Y. Sasaki, T. Minamiki, P. Koutnik, P. Anzenbacher, Jr. and S. Tokito, *Chem. Commun.*, 2015, **51**, 17666-17668.
- C. Rullyani, M. Shellaiah, M. Ramesh, H.-C. Lin and C.-W. Chu, *Org. Electron.*, 2019, **69**, 275-280.
- R. Mitobe, Y. Sasaki, W. Tang, Q. Zhou, X. Lyu, K. Ohshiro, M. Kamiko and T. Minami, *ACS Appl. Mater. Interfaces*, 2022, **14**, 22903-22911.
- H. Shen, Y. Zou, Y. Zang, D. Huang, W. Jin, C.-a. Di and D. Zhu, *Mater. Horiz.*, 2018, **5**, 240-247.
- T. Minamiki, T. Minami, P. Koutnik, P. Anzenbacher, Jr. and S. Tokito, *Anal. Chem.*, 2016, **88**, 1092-1095.
- X. Ji, P. Zhou, L. Zhong, A. Xu, A. C. O. Tsang and P. K. L. Chan, *Adv. Sci.*, 2018, **5**, 1701053.
- H. Fan, Y. Sasaki, Q. Zhou, W. Tang, Y. Nishina and T. Minami, *Chem. Commun.*, 2023, **59**, 2425-2428.
- K. Ohshiro, Y. Sasaki, Q. Zhou, P. Didier, T. Nezaki, T. Yasuie, M. Kamiko and T. Minami, *Chem. Commun.*, 2022, **58**, 5721-5724.
- G. M. Credo, X. Su, K. Wu, O. H. Elibol, D. J. Liu, B. Reddy, T.-W. Tsai, B. R. Dorvel, J. S. Daniels, R. Bashir and M. Varma, *Analyst*, 2012, **137**, 1351-1362.
- Y. Wang, L. Gan, H. Chen, S. Dong and J. Wang, *J. Phys. Chem. B*, 2006, **110**, 20418-20425.
- U. Jarocka, R. Sawicka, A. Góra-Sochacka, A. Sirko, W. Dehaen, J. Radecki and H. Radecka, *Sens. Actuators B Chem.*, 2016, **228**, 25-30.
- Y. Xue, X. Li, H. Li and W. Zhang, *Nat. Commun.*, 2014, **5**, 4348.
- B. de Boer, M. M. Frank, Y. J. Chabal, W. Jiang, E. Garfunkel and Z. Bao, *Langmuir*, 2004, **20**, 1539-1542.
- A. W. Snow, E. E. Foos, M. M. Coble, G. G. Jernigan and M. G. Ancona, *Analyst*, 2009, **134**, 1790-1801.
- T. Y. B. Leung, M. C. Gerstenberg, D. J. Lavrich, G. Scoles, F. Schreiber and G. E. Poirier, *Langmuir*, 2000, **16**, 549-561.
- D. Olson, N. Hopper and W. T. Tysoe, *Surf. Sci.*, 2020, **702**, 121717.
- K. V. G. K. Murty, M. Venkataramanan and T. Pradeep, *Langmuir*, 1998, **14**, 5446-5456.
- H. Klauk, U. Zschieschang, J. Pflaum and M. Halik, *Nature*, 2007, **445**, 745-748.
- I. McCulloch, M. Heeney, C. Bailey, K. Genevicius, I. MacDonald, M. Shkunov, D. Sparrowe, S. Tierney, R. Wagner, W. Zhang, M. L. Chabinyc, R. J. Kline, M. D. McGehee and M. F. Toney, *Nat. Mater.*, 2006, **5**, 328-333.
- Z. Shen, J. Dai, J. Xiong, X. He, W. Mo, B. Hu, N. Sun and X. Hu, *Adv. Synth. Catal.*, 2011, **353**, 3031-3038.
- A. Tada, Y. Geng, M. Nakamura, Q. Wei, K. Hashimoto and K. Tajima, *Phys. Chem. Chem. Phys.*, 2012, **14**, 3713-3724.
- S. Fahn and G. Cohen, *Ann. Neurol.*, 1992, **32**, 804-812.
- N. G. N. Milton, *Drugs Aging*, 2004, **21**, 81-100.
- D. J. Lefter and D. N. Granger, *Am. J. Med.*, 2000, **109**, 315-323.
- G. Jönsson and L. Gorton, *Electroanalysis*, 1989, **1**, 465-468.
- M.-J. Song, S. W. Hwang and D. Whang, *Talanta*, 2010, **80**, 1648-1652.
- J. N. Miller and J. C. Miller, *Statistics and Chemometrics for Analytical Chemistry*, Pearson/Prentice Hall, 2005.
- B. Rani, A. Agarwala, D. Behera, V. P. Verma, A. P. Singh and R. Shrivastava, *Dyes Pigm.*, 2021, **194**, 109596.
- K. Xu, L. He, X. Yang, Y. Yang and W. Lin, *Analyst*, 2018, **143**, 3555-3559.
- E. V. Lampard, A. C. Sedgwick, X. Sun, K. L. Filer, S. C. Hewins, G. Kim, J. Yoon, S. D. Bull and T. D. James, *Chemistryopen*, 2018, **7**, 262-265.
- E. Aparicio-Martínez, A. Ibarra, I. A. Estrada-Moreno, V. Osuna and R. B. Dominguez, *Sens. Actuators B Chem.*, 2019, **301**, 127101.
- E. I. Iwuoha, A. Rock and M. R. Smyth, *Electroanalysis*, 1999, **11**, 367-373.
- C. Hackenberg, R. Kern, J. Hüge, L. J. Stal, Y. Tsuji, J. Kopka, Y. Shiraiwa, H. Bauwe and M. Hagemann, *Plant Cell*, 2011, **23**, 2978-2990.

